



*Journal of Engineering for Development*, Vol. 13(2), December (2021) pp.67-76

**NUMERICAL SOLUTION OF THE DIFFUSIVITY EQUATION FOR DETERMINING  
THE PRODUCTION RATE AND CUMULATIVE PRODUCTION IN THE INFINITE  
ACTING REGIME**

**<sup>1</sup>Erhunmwun, I.D., <sup>2</sup>Amiolemhen, P.E. and <sup>3</sup>Saliu, M.I.**

<sup>1,2,3</sup>Department of Production Engineering, University of Benin, Benin City.

<sup>1</sup>iredia.erhunmwun@uniben.edu <sup>2</sup>patrick.amiolemhen@uniben.edu

<sup>3</sup>mohammed\_saliu@yahoo.com

---

**Abstract**

*This work investigate the well production rate and cumulative production in a circular reservoir. The diffusivity equation was used in the analysis. The work covers infinite acting period of the unsteady flow regime. The finite element technique, using Lagrange quadratic shape elements was employed to carry out the analysis over the cross-section of the reservoir. The analysis was done with the assumption that before the well begins production, there was uniform distribution of pressure all through the reservoir. The results obtained were compared with the result obtained by Christine. The comparison shows a strong agreement between the two methods. Also, Christine solutions only state the production rate and cumulative production of the reservoir at a particular time but this work predicts the production rate and cumulative production in the entire reservoir at the same time.*

---

**Keywords:** Diffusivity equation, infinite acting regime, cumulative production, production rate

Article Information:

Received 24 November, 2021

Revised 08 December, 2021

Accepted 10 December, 2021

Available online 08 March, 2022

## 1.0. Introduction

The diffusivity equation has been solved in dimensionless form (Lee and Wattenbarger, 1996). Chakrabarty et al. (1993) provided a quantitative analysis of the effects of neglecting the quadratic gradient term in solving the diffusion equation governing the transient state. It should be noted that among the flow regimes in reservoir, the transient flow was the most significant state upon which such important characteristics such as permeability, reservoir capacity, and skin factor can be determined using well test analysis (Van Everdingen, 1953; Lee, 1992).

Zainal and Yee (2010) presented the gas–liquid diffusivity measurement and its applications to the transient shut-in modelling. Qanbari and Clarkson (2013) consider a new method for production data analysis of tight and shale gas reservoirs during transient linear flow period. Gandomkar et al. (2014) presented a new numerical scheme based on Orthogonal Collocation (OC) method to solve the diffusivity equation for heterogeneous and homogeneous gas reservoirs.

Barreto and Peres (2012) developed a nonlinear hydraulic diffusivity equation that governs the flow of compressible fluids in porous media. In their study, a general solution that properly accounts for both fluid property behaviour and variable rate was presented. The proposed solution, which was derived from the Green’s-function method by recasting the effect of the viscosity-compressibility product variation as a nonlinear source term, can handle variable gas rate for several well-reservoir geometries of practical interest.

Reza et al. (2016) made a comparison between analytical and numerical solution for both linear and nonlinear diffusivity equation. Secondly, a comprehensive sensitivity analysis was done to find the significant physical properties of reservoir which influence the pressure drop. They also did a comprehensive analysis of parameters such as depletion time, reservoir radius and production rate to find where the pressure differences of linear and non-linear diffusivity equations were significant. In all the methods x-rayed so far, none of the methods has been able to look holistically at the dimensionless cumulative production and production rate, hence, the need for this work.

## 2.0. Methodology

The diffusivity equation can be used to determine the flow properties in a circular reservoir. This equation is as shown in eq. 1 below.

$$\frac{\partial^2 P_D}{\partial r_D^2} + \frac{1}{r_D} \frac{\partial P_D}{\partial r_D} = \frac{\partial P_D}{\partial t_D} \quad (1)$$

and the initial and boundary conditions become:

1. Dimensionless initial condition:

$$\text{Uniform pressure in the reservoir} \quad P_D(r_D, t_D = 0) \leq 0 \quad (2)$$

2. Dimensionless Inner Boundary Condition:

$$\text{Constant rate at the well} \quad \frac{\partial P_D}{\partial r_D}(1, t_D) = 1 \quad (3)$$

3. Dimensionless Outer Boundary Conditions:

- a. “Infinite Acting” Reservoirs

No reservoir boundary  $P_D = (r_D \rightarrow \infty, t_D) = 0$  (4)

b. “No Flow” boundary:

No flux across the reservoir  $\frac{\partial P_D}{\partial r_D}(r_{eD}, t_D) = 0$  (5)

c. Constant Pressure Boundary:

Constant pressure outer boundary  $P_D(r_{eD}, t_D) = 0$  (6)

Eq. 1 can also be written in a condensed form as:

$$\frac{1}{r_D} \frac{\partial}{\partial r_D} \left( r_D \frac{\partial P_D}{\partial r_D} \right) = \frac{\partial P_D}{\partial t_D} \quad (7)$$

In the analysis involving Finite Element method, the governing equation can only be solved if it is in order one. But the governing equation for the diffusivity equation is in order two, so, the need to weaken the governing equation to order one. This is followed by the introduction of the interpolation functions to enable us derive the finite element model. This model is used to generate the elemental matrices and finally assembled to represent the entire domain of the reservoir. The assembled matrix cannot be solved directly. But with the introduction of either the boundary condition or initial conditions or a combination of both the initial and boundary conditions, the nodal values of the parameter can be determined. These procedures were followed and eq. 7 becomes:

$$[K_{ij}^e] \{P_D\} + [M_{ij}^e] \left\{ \dot{P}_{Dj} \right\} = \{Q_i^e\} \quad (8)$$

Eq. 8 is the developed finite element model of the diffusivity equation under the unsteady state flow regime.

where  $K_{ij}^e = \int_{r_{DA}}^{r_{DB}} r_D \frac{d\psi_i^e}{dr_D} \frac{d\psi_j^e}{dr_D} dr_D$  (9)

$$M_{ij}^e = \int_{r_{DA}}^{r_{DB}} r_D \psi_i^e \psi_j^e dr_D \quad (10)$$

Using Quadratic Lagrange Interpolation functions for a quadratic element:

$$\psi_1(r_D) = \frac{1}{h_e^2} (h_e + r_{DA} - r_D)(h_e - 2r_D + 2r_{DA}) \quad (11)$$

$$\psi_2(r_D) = \frac{4}{h_e^2} (r_D - r_{DA})(h_e + r_{DA} - r_D) \quad (12)$$

$$\psi_3(r_D) = \frac{-1}{h_e^2} (r_D - r_{DA})(h_e - 2r_D + 2r_{DA}) \quad (13)$$

### 2.1. Time approximation for Conductive Heat Transfer Model

In this section, we use the already developed finite element model of one-dimensional time-dependent problem to describe time approximation schemes and also convert the ordinary differential equation in time to algebraic equation.

The most commonly used method for solving eq. 8 is the  $\alpha$  family of interpolation in which a weighted average of the time derivative of the dependent variable is approximated to two consecutive time steps by linear interpolation of the values of the variables of the two steps.

For a given time step  $s$ , eq. 8 becomes

$$\left[ K_{ij}^e \right] \{ P_D \}_s + \left[ M_{ij}^e \right] \left\{ \dot{P}_{Dj} \right\}_s = \{ Q_i^e \}_s \quad (14)$$

For the next time step  $s+1$ , eq. 8 becomes

$$\left[ K_{ij}^e \right] \{ P_D \}_{s+1} + \left[ M_{ij}^e \right] \left\{ \dot{P}_{Dj} \right\}_{s+1} = \{ Q_i^e \}_{s+1} \quad (15)$$

Multiply eq. 14 by  $(1-\alpha)$  and eq. 15 by  $\alpha$ , then we add the two resulting equations, we have

$$\left[ M_{ij}^e \right] \left[ (1-\alpha) \left\{ \dot{P}_{Dj} \right\}_s + \alpha \left\{ \dot{P}_{Dj} \right\}_{s+1} \right] + \left[ K_{ij}^e \right] \left[ (1-\alpha) \{ P_D \}_s + \alpha \{ P_D \}_{s+1} \right] = (1-\alpha) \{ Q_i^e \}_s + \alpha \{ Q_i^e \}_{s+1} \quad (16)$$

The  $\alpha$  family of interpolation for time consideration is given as:

$$(1-\alpha) \left\{ \dot{P}_{Dj} \right\}_s + \alpha \left\{ \dot{P}_{Dj} \right\}_{s+1} = \frac{\{ P_{Dj} \}_{s+1} - \{ P_{Dj} \}_s}{\Delta t_{s+1}} \quad (17)$$

Substitute eq. 17 into eq. 16 and using the Crank-Nicholson Scheme where  $\alpha = 1/2$ ,

$$\left[ \left[ M_{ij}^e \right] + \frac{\Delta t_{s+1}}{2} \left[ K_{ij}^e \right] \right] \{ P_{Dj} \}_{s+1} = \left[ \left[ M_{ij}^e \right] - \frac{\Delta t_{s+1}}{2} \left[ K_{ij}^e \right] \right] \{ P_{Dj} \}_s + \frac{\Delta t_{s+1}}{2} \left[ \{ Q_i^e \}_s + \{ Q_i^e \}_{s+1} \right] \quad (18)$$

Substituting the initial condition, we have:

$$\left\{ \bar{Q}_i^e \right\} = \left[ \frac{1}{\Delta t_1} \left[ M_{ij}^e \right] + \frac{1}{2} \left[ K_{ij}^e \right] \right] \{ P_{Dj} \}_1 - \left[ \frac{1}{\Delta t_1} \left[ M_{ij}^e \right] - \frac{1}{2} \left[ K_{ij}^e \right] \right] \{ P_{Dj} \}_0 \quad (19)$$

### 3.0. Results and Discussion

Infinite acting radial flow is common in reservoir and data in the radial flow regime can be used to estimate formation permeability and skin factor. Common situations in which radial flow occurs include flow into vertical wells after wellbore storage effect has ceased and before boundary effects, hydraulically fractured wells after the transient has moved beyond the tips of the fractured horizontal wells before the transient has reached the top and bottom of the productive interval and horizontal wells after the transient has moved beyond the ends of the wellbore.

#### 3.1. Dimensionless production rate against dimensionless time

When a well is put on production with the assumption that the well is producing at a constant wellhead pressure after a shut-in period, the dimensionless production rate in the wellbore begins to drop due to the withdrawal of the fluid from the reservoir through the well bore. The influence of the reservoir boundaries or the shape of the drainage area at this point does not have any effect on the dimensionless production rate in the formation. **That is why the transient state flow is also called the infinite acting state.** During this period, the external boundary of the reservoir is assumed mathematically to be at infinity i.e.,  $r_{eD} \rightarrow \infty$ . This means that the value of the dimensionless production rate is not affected by the external reservoir boundary but only a function

of the dimensionless time  $t_D$ . At this point, it is important to note that in actual sense, the external boundary of the reservoir is not at infinity. During the infinite acting period, the declining rate of the dimensionless production rate through the reservoir is determined by reservoir and fluid characteristics. These characteristics include porosity,  $\phi$  permeability,  $k$ , total compressibility,  $c_t$  and the fluid viscosity,  $\mu$ .

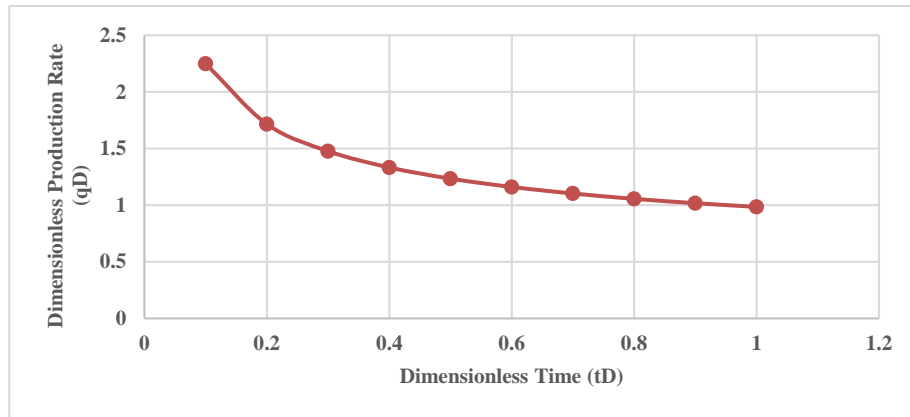


**Fig. 1: A graph of  $q_D$  against  $t_D$  for small  $t_D$  values**

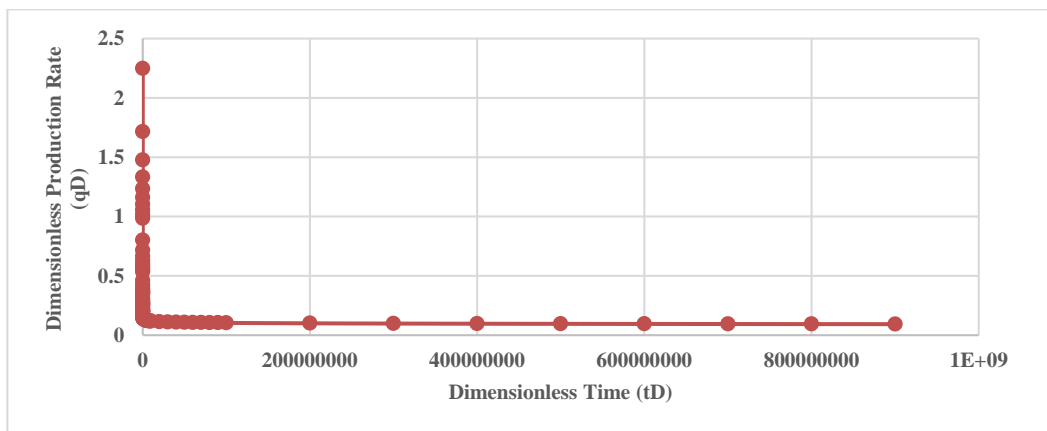


**Fig. 2: A graph of  $q_D$  against  $t_D$  for large  $t_D$  values**

Graphs of dimensionless production rate against dimensionless time from results obtained from the FEM analysis in the infinite acting reservoirs are shown in Figs. 1 and 2. These were shown for different dimensionless times ranges of between 0.0 to 1.0 and 0 to 1000000000 respectively. From Figs. 1 and 2, it was observed that before the reservoir starts production, i.e.,  $t_D = 0$ , the dimensionless pressure was zero in the entire reservoir. This means that before production, the initial pressure in the entire reservoir was constant. As production begins, the dimensionless production rate increases drastically at the early stage. This sudden decrease in the dimensionless production rate was as a result of the expansion of the fluid in the reservoir. Later on, the dimensionless production rate increases almost uniformly with a small slope. This is due to the fact that the fluid which has been withdrawn from the reservoir has been recharged mainly because of the expansion of the compressed fluid within the reservoir.

The results presented in Figs. 1 and 2 are the dimensionless production rate at the well bore of the reservoir at different dimensionless time. The result from this work (FEM) was seen to agree with results published by Christine (1979). To test for the level of convergence of the results, a table of percentage error was generated. These are shown in Table 1.

**Table 1: Percentage Error Comparison between this work (Finite Element Method) and Christine (1979)**

$t_D$	Christine( $q_D$ )	FEM( $q_D$ )	% Error				
0.1	2.2489	2.245567	0.148221	900	0.25421	0.252543	0.655626
0.2	1.7153	1.711967	0.194329	1000	0.25097	0.250637	0.132818
0.3	1.4764	1.473067	0.225774	2000	0.23151	0.231177	0.143982
0.4	1.3326	1.329267	0.250138	3000	0.22142	0.221087	0.150543
0.5	1.2336	1.230267	0.270212	4000	0.21477	0.214437	0.155205
0.6	1.1601	1.156767	0.287332	5000	0.20986	0.209527	0.158836
0.7	1.1025	1.099167	0.302343	6000	0.20602	0.205687	0.161797
0.8	1.0553	1.051967	0.315866	7000	0.20287	0.202537	0.164309
0.9	1.0169	1.013567	0.327794	8000	0.20022	0.199887	0.166484
1	0.98393	0.980597	0.338777	9000	0.19794	0.197607	0.168401
2	0.80063	0.797297	0.416339	10000	0.19594	0.195607	0.17012
3	0.71624	0.712907	0.465393	20000	0.18371	0.183543	0.090723
4	0.66443	0.661097	0.501683	30000	0.17722	0.177053	0.094045
5	0.62821	0.624877	0.530608	40000	0.17209	0.171923	0.096849
6	0.60091	0.597577	0.554714	50000	0.16966	0.169493	0.098236
7	0.5793	0.575967	0.575407	60000	0.16712	0.166953	0.099729
8	0.5616	0.558267	0.593542	70000	0.16502	0.164853	0.100998
9	0.54671	0.543377	0.609708	80000	0.16325	0.163083	0.102093
10	0.53394	0.530607	0.62429	90000	0.16172	0.161553	0.103059
20	0.46116	0.457827	0.722815	100000	0.16037	0.160203	0.103926
30	0.42612	0.422787	0.782252	200000	0.15203	0.151997	0.021925
40	0.40399	0.400657	0.825103	300000	0.14753	0.147497	0.022594
50	0.3882	0.384867	0.858664	400000	0.1445	0.144467	0.023068
60	0.37609	0.372757	0.886313	500000	0.14223	0.142197	0.023436
70	0.36638	0.363047	0.909802	600000	0.14043	0.140397	0.023737
80	0.35833	0.354997	0.930241	700000	0.13894	0.138907	0.023991
90	0.35149	0.348157	0.948344	800000	0.13767	0.137637	0.024212
100	0.34557	0.328903	4.82295	900000	0.13658	0.136547	0.024406
200	0.31081	0.309143	0.536233	1000000	0.13561	0.135577	0.02458
300	0.29335	0.291683	0.56815	2000000	0.12957	0.129553	0.012863
400	0.28204	0.280373	0.590933	3000000	0.12628	0.126263	0.013198
500	0.27382	0.272153	0.608672	4000000	0.12405	0.124033	0.013435
600	0.26744	0.265773	0.623193	5000000	0.12237	0.122353	0.01362
700	0.26226	0.260593	0.635502	6000000	0.12103	0.121013	0.013771
800	0.25792	0.256253	0.646195	7000000	0.11992	0.119903	0.013898
				8000000	0.11897	0.118953	0.014009

9000000	0.11815	0.118133	0.014106	400000000	0.096612	0.09661	0.001725
10000000	0.11742	0.117403	0.014194	500000000	0.095586	0.095584	0.001744
20000000	0.11286	0.112857	0.002954	600000000	0.094764	0.094762	0.001759
30000000	0.11035	0.110347	0.003021	700000000	0.09408	0.094078	0.001772
40000000	0.10863	0.108627	0.003069	800000000	0.093495	0.093493	0.001783
50000000	0.10734	0.107337	0.003105	900000000	0.092985	0.092983	0.001792
60000000	0.10631	0.106307	0.003135				
70000000	0.10545	0.105447	0.003161				
80000000	0.10471	0.104707	0.003183				
90000000	0.10408	0.104077	0.003203				
100000000	0.10351	0.103507	0.00322				
200000000	0.099943	0.099941	0.001668				
300000000	0.097967	0.097965	0.001701				

### 3.2. Dimensionless cumulative production against dimensionless time

Graphs showing the variation in dimensionless production rate against dimensionless time from results obtained from the FEM analysis in the infinite acting reservoirs are shown in Figs. 3 and 4. These were shown for different dimensionless time ranging between 0.0 to 1.0 and 0 to 1000000000 respectively. From Figs. 3 and 4, it was observed that there was a linear increase in dimensionless cumulative production with respect to the dimensionless time. That is to say that as production time increases, the produced fluid also increases which is expected.

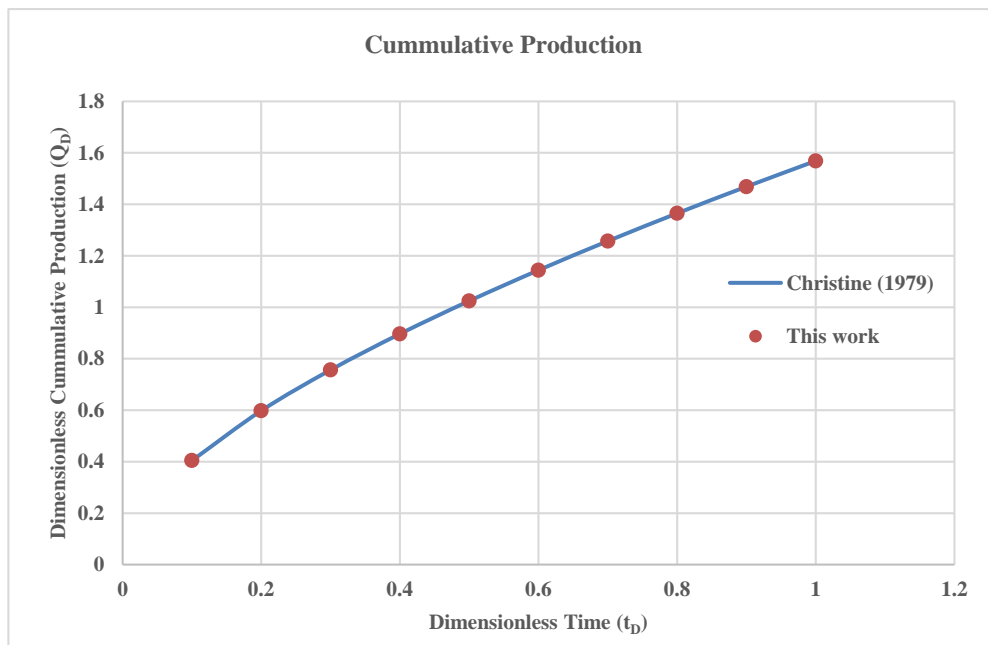
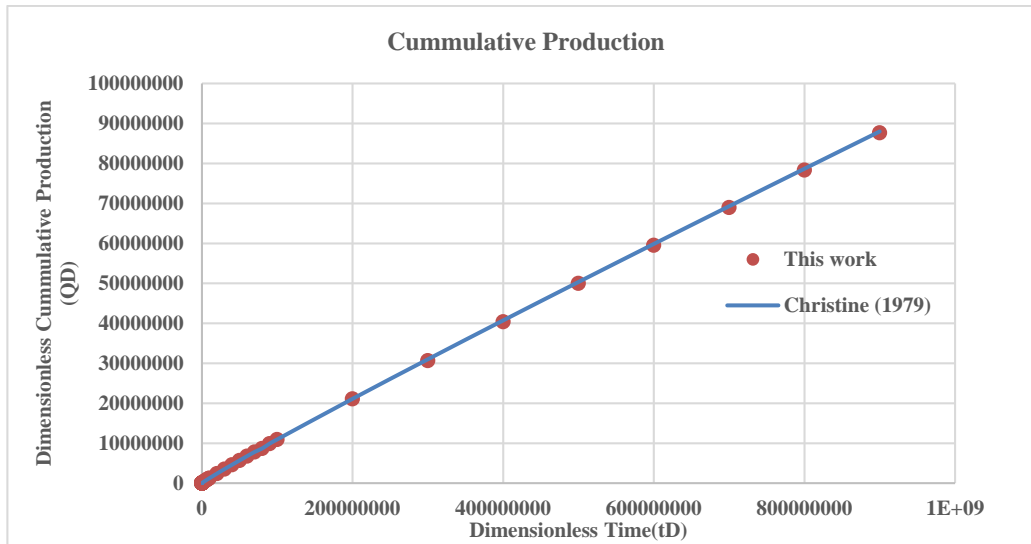


Fig. 3: A graph of  $Q_D$  against  $t_D$  for small  $t_D$  values



**Fig. 4: A graph of  $Q_D$  against  $t_D$  for large  $t_D$  values**

The results presented in Figs. 3 and 4 are the dimensionless cumulative production at the well bore of the reservoir at different dimensionless time. The result from this work (FEM) was seen to agree with results published by Christine (1979). To test for the level of convergence of the results, a table of percentage error was generated. These are shown in Table 2.

**Table 2: Percentage Error Comparison between this work (Finite Element Method) and Christine(1979)**

$t_D$	Christine( $Q_D$ )	FEM( $Q_D$ )	% Error
0.1	2.2489	2.245567	0.148221
0.2	1.7153	1.711967	0.194329
0.3	1.4764	1.473067	0.225774
0.4	1.3326	1.329267	0.250138
0.5	1.2336	1.230267	0.270212
0.6	1.1601	1.156767	0.287332
0.7	1.1025	1.099167	0.302343
0.8	1.0553	1.051967	0.315866
0.9	1.0169	1.013567	0.327794
1	0.98393	0.980597	0.338777
2	0.80063	0.797297	0.416339
3	0.71624	0.712907	0.465393
4	0.66443	0.661097	0.501683
5	0.62821	0.624877	0.530608
6	0.60091	0.597577	0.554714
7	0.5793	0.575967	0.575407
8	0.5616	0.558267	0.593542
9	0.54671	0.543377	0.609708
10	0.53394	0.530607	0.62429
20	0.46116	0.457827	0.722815
30	0.42612	0.422787	0.782252
40	0.40399	0.400657	0.825103
50	0.3882	0.384867	0.858664
60	0.37609	0.372757	0.886313
70	0.36638	0.363047	0.909802
80	0.35833	0.354997	0.930241
90	0.35149	0.348157	0.948344
100	0.34557	0.328903	4.82295
200	0.31081	0.309143	0.536233
300	0.29335	0.291683	0.56815
400	0.28204	0.280373	0.590933
500	0.27382	0.272153	0.608672
600	0.26744	0.265773	0.623193
700	0.26226	0.260593	0.635502
800	0.25792	0.256253	0.646195
900	0.25421	0.252543	0.655626
1000	0.25097	0.250637	0.132818
2000	0.23151	0.231177	0.143982
3000	0.22142	0.221087	0.150543
4000	0.21477	0.214437	0.155205
5000	0.20986	0.209527	0.158836



6000	0.20602	0.205687	0.161797
7000	0.20287	0.202537	0.164309
8000	0.20022	0.199887	0.166484
9000	0.19794	0.197607	0.168401
10000	0.19594	0.195607	0.17012
20000	0.18371	0.183543	0.090723
30000	0.17722	0.177053	0.094045
40000	0.17209	0.171923	0.096849
50000	0.16966	0.169493	0.098236
60000	0.16712	0.166953	0.099729
70000	0.16502	0.164853	0.100998
80000	0.16325	0.163083	0.102093
90000	0.16172	0.161553	0.103059
100000	0.16037	0.160203	0.103926
200000	0.15203	0.151997	0.021925
300000	0.14753	0.147497	0.022594
400000	0.1445	0.144467	0.023068
500000	0.14223	0.142197	0.023436
600000	0.14043	0.140397	0.023737
700000	0.13894	0.138907	0.023991
800000	0.13767	0.137637	0.024212
900000	0.13658	0.136547	0.024406
1000000	0.13561	0.135577	0.02458
2000000	0.12957	0.129553	0.012863
3000000	0.12628	0.126263	0.013198
4000000	0.12405	0.124033	0.013435
5000000	0.12237	0.122353	0.01362
6000000	0.12103	0.121013	0.013771
7000000	0.11992	0.119903	0.013898
8000000	0.11897	0.118953	0.014009
9000000	0.11815	0.118133	0.014106
10000000	0.11742	0.117403	0.014194
20000000	0.11286	0.112857	0.002954
30000000	0.11035	0.110347	0.003021
40000000	0.10863	0.108627	0.003069
50000000	0.10734	0.107337	0.003105
60000000	0.10631	0.106307	0.003135
70000000	0.10545	0.105447	0.003161
80000000	0.10471	0.104707	0.003183
90000000	0.10408	0.104077	0.003203

#### 4.0. Conclusion

In this research, we have formulated the finite element based model for the diffusivity equation under the infinite acting flow regime. The result obtained were used to analyse the production rate and cumulative production for different radii and time. Under the unsteady state flow regime, the dimensionless flow rate and dimensionless cumulative production was seen to vary radially and also with time. The accuracy of the results was validated by comparing the results with existing results in literature. The result from this research shows a strong agreement between the results with existing results in literature.

Finally, the accuracy of the results obtained was admissible and it therefore shows that the Finite element method can be used in approximating the dimensionless production rate and cumulative production values of fluid in circular reservoirs under various conditions of steady state, pseudo steady state and the unsteady state flow regime.

#### References

- Barreto, A.B. and Peres, A.M. (2012). *A variable-rate solution to the nonlinear diffusivity gas equation by use of green's-function method*. SPE 145468.
- Chakrabarty, C., Ali S. and Tortike W. (1993). *Analytical solutions for radial pressure distribution including the effects of the quadratic gradient term*. *Water Resour Res*, 29(4), pp. 1171–1177.
- Gandomkar, A., Rahimpour, M.R. and Jahanmiri, A. (2014). *Applying a new method to solve diffusivity equation for gas reservoirs*. *J. Petrol. Sci. Eng.*, pp. 1 – 8.
- Lee, W.J. and Wattenbarger R.A. (1996). *Gas reservoir engineering*, SPE Textbook Series, Vol. 5. Society of Petroleum Engineers, pp. 349.
- Qanbari, F., and C. R. Clarkson. (2013) "Analysis of Transient Linear Flow in Tight Oil and Gas Reservoirs with Stress-Sensitive Permeability and Multi-Phase Flow." Paper presented at the SPE Unconventional Resources Conference Canada, Calgary, Alberta, Canada. doi: <https://doi.org/10.2118/167176-MS>
- Reza, A., Mohamad, M. and Zahra, S. (2016). *Parametric analysis of diffusivity equation in oil reservoirs*, *J Petrol Explor Prod Technol*, 6, pp. 1-11.
- Van Everdingen, A. (1953). *The skin effect and its influence on the productive capacity of a well*. *J Petrol Techn.*, 5(06), pp. 171–176.
- Zainal, S. and Yee, H.V. (2010). *Gas-diffusivity measurement in reservoir fluid at elevated pressures systems for transient shut-in modelling*. In: SPE Latin American and Caribbean Petroleum Engineering Conference. SPE 139004.